THIELE CENTRE
FOR APPLIED MATHEMATICS IN NATURAL SCIENCE

To be and not to be: scale correlations in random multifractal processes

Jochen Cleve, Jürgen Schmiegel and Martin Greiner

Research Report

No. 07 I May 2006

To be and not to be: scale correlations in random multifractal processes

This Thiele Research Report is also Research Report number 476 in the Stochastics Series at Department of Mathematical Sciences, University of Aarhus, Denmark.

To be and not to be: scale correlations in random multifractal processes

Jochen Cleve,[1] Jürgen Schmiegel,[2] and Martin Greiner[3]

[1] *Untere Weidenstraße 21, D–81543 München, Germany**

[2] *Thiele Centre for Applied Mathematics in Natural Science, Aarhus University, DK-8000 Aarhus, Denmark*†

[3] *Corporate Technology, Information&Communications, Siemens AG, D-81730 München, Germany*‡

(Dated: May 16, 2006)

We discuss various properties of a random multifractal process, which are related to the issue of scale correlations. By design, the process is homogeneous, non-conservative and has no built-in scale correlations. However, when it comes to observables like breakdown coefficients, which are based on a coarse-graining of the multifractal field, scale correlations do appear. In the log-normal limit of the model process, the conditional distributions and moments of breakdown coefficients reproduce the observations made in fully developed small-scale turbulence. These findings help to understand several puzzling empirical details, which have been extracted from turbulent data already some time ago.

PACS numbers: 47.27.Eq, 47.27.Gs, 02.50.Ey

Keywords: small-scale turbulence, turbulence modeling, multifractality, breakdown coefficients, Kramers-Moyal coefficients

I. INTRODUCTION

It is always nice to have a good model. As a theoretical physicist you exactly know what you put in. Then you can start repeating to do the same things experimentalists do with their data and begin to understand things which have been empirically described before, but have remained obscure, or even mystical.

Take fully developed turbulence as an example. Deviations from the pioneering K41 scaling prediction [1] are well described with the multifractal formalism and have lead to the empirical modeling of the turbulent energy cascade with random multiplicative cascade processes [2]. By design, the random multiplicative transfer of energy flux from the integral down to the dissipation scale comes with no scale correlations. However, this model property has not been confirmed in a first data inspection based on breakdown coefficients of the energy dissipation [3, 4]. Another, Markovian-based approach [5, 6] supports this finding, that the turbulent energy cascade appears to come with inherent scale correlations. It is exactly this conflict which motivates us to look closer into the nature of scale correlations of random multifractal processes in general.

*Electronic address: jochen_cleve@web.de

†Electronic address: schmiegl@imf.au.dk

‡Electronic address: martin.greiner@siemens.com

Previous work in this direction has focused on binary discrete random multiplicative cascade processes. Their non-conservative variants were able to explain the observed scale-independent unconditional distributions of breakdown coefficients [3, 4] as fixed points resulting from small-scale resummation [7, 8], which are also different from the employed cascade generator. Furthermore, by adopting an experimentalist's view, who is not aware of the underlying binary-tree hierarchy of the cascade process and who then homogeneously samples observables, the correlations observed in the conditional distributions of breakdown coefficients [3, 4] could be reproduced, especially when the cascade generator is chosen to be positively skewed [9]. With the same overall approach, also the observed scale-dependence of Kramers-Moyal coefficients, representing the Markovian route to the turbulent energy cascade [5, 6], could be qualitatively reproduced [10].

So far the qualitative success to explain the observed scale correlations out of non-scale-correlated models is tied to the binary discrete random multiplicative cascade processes. Of course, this is subject to some criticism. First of all, the turbulent energy cascade is neither binary nor discrete. Second, although plausible from a physics perspective, the employed small-scale resummation as well as the experimentalist's homogeneous sampling appear to be operationally rather ad hoc. In this respect it would be nice to consider more general and more elegant stochastic processes, which are not in need of ad hoc operations, and which hopefully not only confirm the previous findings, but also put them on more firm ground and, maybe, also allow to resolve some more of the empirically observed and quantified puzzling details.

This is exactly what we are going to demonstrate. In Ref. [11] an elegant stochastic energy-cascade process has been proposed, which is continuous, homogeneous and causal. It delivers multifractality by design. This random multifractal process, which will be briefly presented in Sect. II, does not have built-in scale correlations, but, as we will see in Sects. III and IV, when it comes to the analysis of breakdown coefficients and Kramers-Moyal coefficients the scale correlations do appear again. The precision reached within these simulations allows for several further quantitative statements: (i) the obtained distributions of breakdown coefficients allow no room for log-stable statistics of the energy dissipation, except when close to the log-normal limit; (ii) extracted moments of breakdown coefficients reproduce the puzzling systematics on apparent scaling exponents, observed and discussed in Refs. [4, 12]; (iii) the two differing outcomes of the extracted Kramers-Moyal coefficients [5, 6], which trace back to different operational definitions, are reproduced; (iv) the intermittency exponent can be extracted from the first Kramers-Moyal coefficient. A conclusion and outlook will be given in Sect. V.

II. MODELING OF A CONTINUOUS AND HOMOGENEOUS RANDOM MULTIFRACTAL PROCESS

In Ref. [11], see Refs. [13–17] for related approaches, a positive-valued multifractal field $\varepsilon(x,t)$ on continuous 1+1 space-time has been designed as the stochastic integral

$$\varepsilon(x,t) = \exp\left\{\int_{t-T}^{t} dt' \int_{x-g(t-t')}^{x+g(t-t')} dx' \gamma(x',t')\right\} \ . \tag{1}$$

By assumption $\gamma(x,t) \sim S_\alpha((dxdt)^{\alpha^{-1}-1}\sigma, -1, \sigma^\alpha/\cos(\pi\alpha/2))$ is a Lévy-stable white-noise field [18] with property $\langle\exp\{\gamma\}\rangle = 1$. The causality cone

$$g(t-t') = \frac{L}{2}\min\left\{\left(1+\frac{(L-\eta)}{\eta}\frac{(T-\Delta T-(t-t'))}{(T-\Delta T)}\right)^{-1}\ ,\ 1\right\} \tag{2}$$

has the properties $g(T-\Delta T) = g(T) = L/2$ and $g(0) = \eta/2$, with $L \gg \eta$ representing the integral and dissipation length, and $T \gg \Delta T$ the integral time and a convenient cutoff. The explicit shape (2) allows to interpret the field (1) as a product of independently and identically distributed random weights $q(l_j)$,

$$\varepsilon(x,t) \sim \prod_{j=1}^{J}\exp\left\{\int_{t-t_{j-1}}^{t-t_j}dt'\int_{x-g(t-t')}^{x+g(t-t')}dx'\,\gamma(x',t')\right\} \equiv \prod_{j=1}^{J} q(l_j)\ , \tag{3}$$

which belong to the hierarchy of scales $l_j = L/\lambda^j = 2g(T-t_j)$ confined by $\eta = l_J$ and $L = l_0$. This reflects the spirit of random multiplicative cascade processes and demonstrates that no scale correlations are build into the ansatz (1). Furthermore, with the setting $\Delta T/T = \eta/L$ Eqs. (1) and (2) directly lead to perfect scaling of the two-point correlation densities

$$\frac{\langle\varepsilon^{n_1}(x_1,t)\varepsilon^{n_2}(x_2,t)\rangle}{\langle\varepsilon^{n_1}(x_1,t)\rangle\langle\varepsilon^{n_2}(x_2,t)\rangle} = \left(\frac{L}{|x_2-x_1|}\right)^{\tau_{n_1+n_2}-\tau_{n_1}-\tau_{n_2}} \tag{4}$$

with two-point distance $\eta \le |x_2-x_1| \le L$. For larger distances the correlations are equal to one. The multifractal scaling exponents are given by $\tau_n = \tau_2(n^\alpha-n)/(2^\alpha-2)$ with $\tau_2 = (\sigma^\alpha/\cos\frac{\pi\alpha}{2})(2-2^\alpha)\eta T$.

Besides L, T and η, the only other parameters of the stochastic process (1) are the Lévy-stable index $0\le\alpha\le 2$ and σ. In [11] the two latter have been fixed by the observed scaling exponents τ_2 and τ_3 extracted from the lowest-order two-point correlation densities; with no room left for further adjustments the predicted three-point correlation densities have been shown to be in excellent agreement with their counterparts from turbulent energy-dissipation data.

All results presented here are based on model simulations. Parameters are set $L/\eta = 500$ and $T = L$. The resolution $\Delta x = \Delta t = \eta/6$ of the numerical discretization has been checked to produce sufficient convergence. For given α and σ, observables like two-point correlation densities, breakdown coefficients and Kramers-Moyal coefficients are sampled from a simulated equal-time trace $\varepsilon(x)$ of length $L_{\rm trace} = 10^7\eta$. The such sampled lowest-order two-point correlation densities reproduce (4) with high quality.

III. APPARENT SCALE-CORRELATIONS I: BREAKDOWN COEFFICIENTS

The breakdown coefficients

$$b(x;l,\lambda,\Delta) = \frac{\varepsilon_{l/\lambda}(x+l\Delta(\lambda-1)/\lambda)}{\varepsilon_l(x)} \tag{5}$$

are defined as the ratio of coarse-grained field amplitudes

$$\varepsilon_l(x) = \frac{1}{l}\int_{x-l/2}^{x+l/2}\varepsilon(x')dx' \tag{6}$$

at scales l/λ and l, separated by the scale parameter $\lambda > 1$. The parameter Δ describes the relative position between parent and offspring interval. $\Delta = 0$ corresponds to the centered case and $\Delta = \pm 1/2$ to right- and left-alignment, respectively.

For turbulent cascades at high Reynolds numbers, scale-independence of unconditional distributions of breakdown coefficients has been observed in the upper part of the inertial range [3, 4, 19, 20] and has been thought to describe the cascade generator [20–23], allowing for an alternative approach to analyze multifractality. However, by construction the breakdown coefficients (5) are different from the log-stable random multiplicative weights $q(l)$ of (3). This is further emphasized in Fig. 1, which illustrates the unconditional distribution of left/right-sided $\lambda = 2$ breakdown coefficients sampled from simulated model traces. Within the upper cascade regime $20\eta \leq l \leq L$ these distributions are found to be independent of the scale l; for smaller and larger scales they are more narrow. The shown distributions are not of log-stable type; see also Fig. 2. They can be nicely parametrized with a symmetric Beta-distribution $p(b) \sim b^{\beta-1}(2-b)^{\beta-1}$. For the model parameter setting with $\alpha = 2.0$ and $\tau(2) = 0.24$ the found distribution nicely matches the distribution reported in the analysis of a high-Reynolds number atmospheric boundary layer [3].

Upon switching from unconditional to conditional distributions scale correlations do appear. When conditioned onto a large (small) parent breakdown coefficient, the distribution with $\lambda = 2$, $\Delta = \pm 1/2$ of Fig. 2(top left) results to be broader (more narrow) than its unconditional counterpart. This outcome is in full agreement with the experimental findings reported in [3]. Fig. 2(top center) shows the related centered distributions. In its unconditional form it is again well described with a symmetric Beta distribution, but now with increased exponent $\beta = 4.9$. For a large parent breakdown coefficient the distribution is broadened and shifted to the right, whereas it is narrowed and shifted to the left once the parent is small. These findings are in perfect agreement with the experimental observations presented in [4]. This demonstrates that the scale correlations reported in [3, 4] can be fully reproduced by the stochastic process (1), which by construction has no built-in scale correlations. – But where do the scale correlations come from? They trace back to the coarse-graining (6) of the non-conservative multifractal field. This correlates the breakdown coefficient to its parent.

So far only the log-normal limit ($\alpha = 2$) of (1) has been discussed. With the same choice $\tau_2 = 0.24$ for the intermittency exponent, the second and third rows of Fig. 2 illustrate the distributions of $\lambda = 2$ breakdown coefficients for $\alpha = 1.7$ and 1.4, respectively. With decreasing α the differences of the conditional to the unconditional $\Delta = \pm 1/2$ distributions also decrease, leading to a disappearance of the scale correlations at $\alpha \approx 1.4$. Note also another detail for $\alpha < 2$: all distributions increase again as the breakdown coefficient approaches zero (two) from above (below). This effect becomes stronger the smaller α is chosen and is a fingerprint of the excess probability $p(q = 0^+) > 0$ occurring for log-stable distributions; see also the third column of Fig. 2. Also the distributions of centered breakdown coefficients reveal an interesting behavior with α. Whereas for $\alpha = 2$ the left-shifted conditional distribution has a larger maximum than the right-shifted one, the two maxima become about equal for $\alpha = 1.7$ and reverse their order for $\alpha = 1.4$. In comparison with the experimental observations [3, 4] these findings suggest that the stability index α should be two, or at least very close to two. Except for the log-normal limit, this leaves no room for the log-stable modeling of the turbulent energy cascade [24, 25]. Put into a more general context, scale correlations observed in conditional distributions of breakdown coefficients allow for a sensitive parameter estimation of universal multifractals [26]. – For the remainder of this Article

we adopt the limit $\alpha = 2$, where the Lévy-stable white-noise field of (1) corresponds to a non-centered Gaussian white-noise field.

Up to now we have only investigated breakdown coefficients with a scale ratio of $\lambda = 2$, but there is no reason to restrict the analysis to this scale ratio. Model simulations reveal that as for $\lambda = 2$, the distributions of breakdown coefficients for arbitrary $1 < \lambda < 2$ turn out to be scale-independent within the upper part $20\eta \leq l \leq L$ of the cascade range. They can be well described with asymmetric Beta distributions supported on $[0, \lambda]$. Before addressing the issue of scale-correlations within a new context in Sect. IV, we quantify some λ-dependent properties of the unconditional breakdown coefficients.

Fig. 3 shows the second moment $\langle b^2(\lambda, \Delta)\rangle$ of the breakdown coefficients as a function of λ and Δ. They have been calculated for a typical length scale within the observed scale-independent regime $20\eta \leq l \leq L$. If the breakdown coefficients were identical to the random multiplicative weights $q(l; \lambda)$ of Eq. (3), then the modified form

$$\tilde{\tau}_2(\lambda, \Delta) = \ln\langle b^2(\lambda, \Delta)\rangle / \ln \lambda \tag{7}$$

should reproduce the multifractal exponent τ_2, which has served as input into the modeling (1). Evidently this is not the case. The apparent exponent $\tilde{\tau}_2$ strongly depends on Δ and λ. In Ref. [4] the empirical expression

$$\tilde{\tau}_2(\lambda, \Delta) = \tilde{\tau}_2(\Delta) + a(\Delta) \ln\ln \lambda \tag{8}$$

has been found to describe the experimentally observed λ-dependence with reasonable precision. As can be seen in Fig. 3, this expression also fits well to our simulational findings. Fitted parameters are $\tilde{\tau}_2(\Delta = 0) = 0.14$, $a(\Delta = 0) = 0.034$, and $\tilde{\tau}_2(\Delta = \pm 1/2) = 0.196$, $a(\Delta = \pm 1/2) = 0.044$. Neither for $\Delta = 0$ nor for $\Delta = \pm 1/2$ the corrected exponent $\tilde{\tau}_2(\Delta)$ is able to reproduce the true $\tau_2 = 0.24$.

These findings show two things: first, the experimentally observed moment systematics (8) of breakdown coefficients is again fully reproduced by the stochastic process (1), and, second, there is no need to argue which combination λ, Δ is best for the moments of breakdown coefficients to reproduce the correct scaling exponents. As to the latter point, Ref. [12] has conjectured that the best combination is $\lambda = 2$, $\Delta = \pm 1/2$. In fact, another quick look at Fig. 3 reveals that this combination produces an apparent intermittency exponent which comes closest to the true one. Looking again at the construction (1)-(3) of our stochastic process, much better suited observables for the extraction of true multifractal exponents are the two-point correlation densities (4). See also Refs. [27, 28] for related data analysis.

IV. APPARENT SCALE-CORRELATIONS II: KRAMERS-MOYAL COEFFICIENTS

We return to the issue of scale correlations and discuss the moments

$$D_n(\ln \varepsilon_l; l, \lambda, \Delta) = \frac{1}{n! \ln \lambda} \langle (\ln b(l, \lambda, \Delta))^n | \ln \varepsilon_l \rangle \tag{9}$$

of logarithmic breakdown coefficients conditioned on the logarithmic coarse-grained field. For $\Delta = 0$ and a typical length scale, the $1 < \lambda \leq 2$ dependence of the first two moments is shown in Fig. 4. A good empirical parametrization of the simulational results is given by

$$D_1(\ln \varepsilon_l; l, \lambda, \Delta) = a_{10}(l, \Delta) + a_{11}(l, \lambda, \Delta) \left(\ln \varepsilon_l - \langle \ln \varepsilon_l \rangle\right) + \cdots \tag{10}$$

$$D_2(\ln \varepsilon_l; l, \lambda, \Delta) = a_{20}(l, \lambda, \Delta) + a_{21}(l, \lambda, \Delta) \left(\ln \varepsilon_l - \langle \ln \varepsilon_l \rangle\right) + \cdots . \tag{11}$$

All linear D_1 curves are found to intersect at $\ln \varepsilon_l = \langle \ln \varepsilon_l \rangle$, which makes the coefficient a_{10} independent of λ. Already for $\lambda = 2$ the slope a_{11} is positive and increases further, the smaller λ becomes. This positive correlation between logarithmic breakdown coefficient and logarithmic coarse-grained field appears to converge for λ sufficiently close to one. See also Fig. 5a, which illustrates the l dependence of a_{11} for various λ. As for the second-order moment, the slope coefficient a_{21} remains close to zero, being positive (negative) above (below) $\lambda \approx 1.15$. This makes D_2 more or less independent of $\ln \varepsilon_l$, but not of λ. The coefficient a_{20} declines rapidly as λ becomes smaller; see also Fig. 5b.

For comparison, we give the respective unconditional moments of the log-normal random multiplicative weights of Eq. (3):

$$\langle \ln q \rangle / \ln \lambda = -\tau_2/2 \; , \tag{12}$$

$$\langle \ln^2 q \rangle / 2 \ln \lambda = \tau_2/2 + (\tau_2^2/8) \ln \lambda \; . \tag{13}$$

These relations follow straightforwardly from the multifractal sum rules [28], which relate the cumulants of the logarithmic random multiplicative weights to the multifractal exponents. Except for a negligible $2 \geq \lambda > 1$ dependence of (13), the two moments are constant. The comparison of (12)-(13) with (10)-(11) demonstrates again that the breakdown coefficients should not be mixed up with the random multiplicative weights.

However, the comparison of (10) with (12) leaves us with a surprising detail. Fig. 6 illustrates the l dependence of the coefficient a_{10}. The results for $\Delta = 0$ and $\Delta = \pm 1/2$ are almost identical and show only a very weak $\ln l$ dependence. More or less the coefficient is constant and takes on the value $a_{10} \approx -0.12$, which coincides with (12). Without having a deeper explanation at hand, it appears that a_{10} allows to extract the value of the intermittency exponent with reasonable precision. – Due to (13), a similar extraction might also be successful from (11). A glimpse at Fig. 5b destroys this hope. The coefficient a_{20} strongly depends on λ and weakly on l. To some degree it also depends on Δ. Except for $\lambda = 2$, its value is always well below $\tau_2/2 = 0.12$ of (13).

If the moments (9) converge in the limit $\lambda \to 1$, they would become the Kramers-Moyal coefficients of the Markovian description of the turbulent energy cascade [5, 6]. Since any data-driven extraction faces difficulties with this limit, two different operational definitions have been put forward: Ref. [5] uses a relative, l independent truncation at $\lambda_1 = 1.04$, whereas Ref. [6] employs an absolute, but l dependent truncation at $\lambda_2 = l/(l - 4.4\eta)$. We have adopted these two operational definitions with the small modifications $\lambda_1 = 16/15$ and $\lambda_2 = l/(l - 4\eta)$, adopted to our numerical resolution. Fig. 7 illustrates the model-based outcome for the drift coefficient $\gamma(l) = a_{11}(l, \lambda, \Delta = 0)$ and the diffusion coefficient $D(l) = a_{20}(l, \lambda, \Delta = 0)$. The curves corresponding to the λ_1 limit are identical to the $\lambda = 16/15$ curves of Fig. 5; see also Fig. 4, where the two bold curves correspond to the two different limits. In the λ_1 limit, the diffusion coefficient is more or less constant, whereas the drift coefficient increases to some extend with increasing length scale. Although the model has not been fitted to the low-temperature helium-jet data used in Ref. [5], the order of magnitude of the found drift and diffusion coefficient matches well the values $\gamma = 0.21$ and $D = 0.03$ stated in this reference. The λ_2 limit results in an l dependence for the drift as well as the diffusion coefficient, which can be parametrized with $\gamma(l) = 0.012(l/\eta)^{0.51}$ and $D(l) = 0.32(l/\eta)^{-0.62}$. Also shown in Fig. 7 are the expressions $\gamma(l) = 0.32 - 0.05 \ln(L/l)$ and $D(l) = 0.01(L/l)^{0.4}$ of Ref. [6], which again have been extracted from low-temperature helium-jet data. Whereas the functional forms are identical for the diffusion coefficient, the functional forms for the drift coefficient are a little different. However, orders of magnitude

and trends are close by. – Overall, the model findings for both operational definitions of the $\lambda \to 1$ limit are in good qualitative agreement with the experimental results stated in Refs. [5, 6]. This shows that there is no need to argue whether the one definition is more sensitive than the other [6]. Even more important, this demonstrates that the observed scale correlations ($\gamma \neq 0$) and scale-dependence ($\gamma = \gamma(l)$, $D = D(l)$) can not be interpreted as signatures for the turbulent energy cascade to deviate from a scale-independent and scale-uncorrelated multifractal process.

V. CONCLUSION

The scale correlations, appearing in conditional distributions and moments of coarse-grained observables like breakdown coefficients, are not in conflict with random multifractal processes, which have no built-in scale correlations. Given the quantitative agreement reached between the model findings and the results extracted from turbulent data, we are now tempted to claim that these apparent scale-correlations go hand in hand with non-conservative random multifractal processes. The former are a consequence of the latter and have to be there! In this respect, it would be interesting to check on scale correlations in other known multifractal processes, like for example Internet traffic engineering [29] and econophysics [30, 31]. As to fully developed small-scale turbulence, our findings demonstrate that random multifractal processes appear to contain more truth than previously anticipated.

---

[1] A. Kolmogorov, Dokl. Akad. Nauk. SSSR **30**, 301 (1941).
[2] U. Frisch, *Turbulence* (Cambridge University Press, Cambridge, 1995).
[3] K. R. Sreenivasan and G. Stolovitzky, J. Stat. Phys. **78**, 311 (1995).
[4] G. Pedrizzetti, E. Novikov, and A. Praskovsky, Phys. Rev. E**53** p. 475 (1996).
[5] A. Naert, R. Friedrich, and J. Peinke, Phys. Rev. E**56** p. 6719 (1997).
[6] P. Marcq and A. Naert, Physica D**124** p. 368 (1998).
[7] B. Jouault, P. Lipa, and M. Greiner, Phys. Rev. E **59**, 2451 (1999).
[8] B. Jouault, M. Greiner, and P. Lipa, Physica D **136**, 125 (2000).
[9] B. Jouault and M. Greiner, Fractals **10**, 321 (2002).
[10] J. Cleve and M. Greiner, Phys. Lett. A **273**, 104 (2000).
[11] J. Schmiegel, J. Cleve, H. Eggers, B. Pearson, and M. Greiner, Phys. Lett. A **320**, 247 (2004).
[12] M. Nelkin and G. Stolovitzky, Phys. Rev. E **54**, 5100 (1996).
[13] F. Schmitt and D. Marsan, Eur. Phys. J. B **20**, 3 (2001).
[14] F. Schmitt, Eur. Phys. J. B **34**, 85 (2003).
[15] J. Muzy and E. Bacry, Phys. Rev. E **66**, 056121 (2002).
[16] P. Chainais, R. Riedi, and P. Abry, IEEE Trans. Inf. Theory (2003).
[17] P. Chainais, R. Riedi, and P. Abry, Traitement du Signal **22** (2005).
[18] G. Samorodnitsky and M. Taqqu, *Stable non-Gaussian random processes* (Chapman & Hall, New York, 1994).
[19] C. van Atta and T. Yeh, J. Fluid Mech. **71**, 417 (1975).
[20] A. Chhabra and K. Sreenivasan, Phys. Rev. Lett. **68**, 2762 (1992).
[21] E. Novikov, Appl. Math. Mech. **35**, 321 (1971).

[22] E. Novikov, Phys. Fluids A **2**, 814 (1990).
[23] M. Ossiander and E. Waymire, Ann. Statist. **28**, 1533 (2000).
[24] S. Kida, J. Phys. Soc. Japan **60**, 5 (1991).
[25] F. Schmitt, D. Lavallée, D. Schertzer, and S. Lovejoy, Phys. Rev. Lett. **68**, 305 (1992).
[26] D. Schertzer and S. Lovejoy, Physica A **185**, 187 (1992).
[27] J. Cleve, M. Greiner, B. Pearson, and K. Sreenivasan, Phys. Rev. E **69**, 066316 (2004).
[28] J. Cleve, T. Dziekan, J. Schmiegel, O. Barndorff-Nielsen, B. Pearson, K. Sreenivasan, and M. Greiner, Phys. Rev. E **71**, 026309 (2005).
[29] R. H. Riedi, M. S. Crouse, V. J. Ribeiro, and R. G. Baraniuk, IEEE Transactions on Information Theory **45**, 992 (1999).
[30] J. Muzy, J. Delour, and E. Bacry, Eur. Phys. J. B **17**, 537 (2000).
[31] E. Bacry, J. Delour, and J. Muzy, Phys. Rev. E **64**, 026103 (2001).

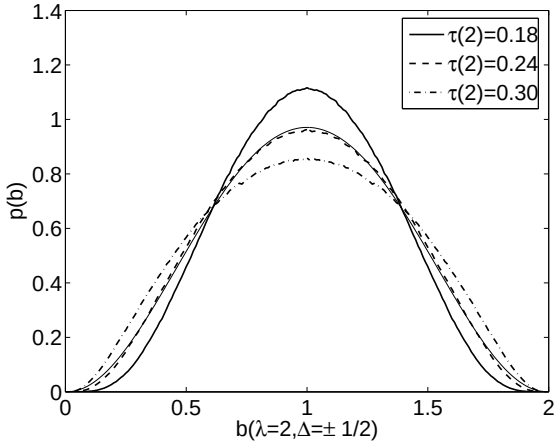

FIG. 1: Unconditional distributions of breakdown coefficients with $\lambda = 2$, $\Delta = \pm 1/2$ at scale $l = 32\eta$ within the scale-independent regime $20\eta < l < L$. They have been sampled from model traces with parameter settings $\alpha = 2.0$ and $\tau(2) = 0.18$ (solid), 0.24 (dashed), 0.30 (dash-dotted). For comparison a symmetric Beta distribution $p(b) \sim b^{\beta-1}(2-b)^{\beta-1}$ with $\beta = 3.2$ is also shown (thin solid), which has been reported in the analysis of a high-Reynolds number turbulent flow [3].

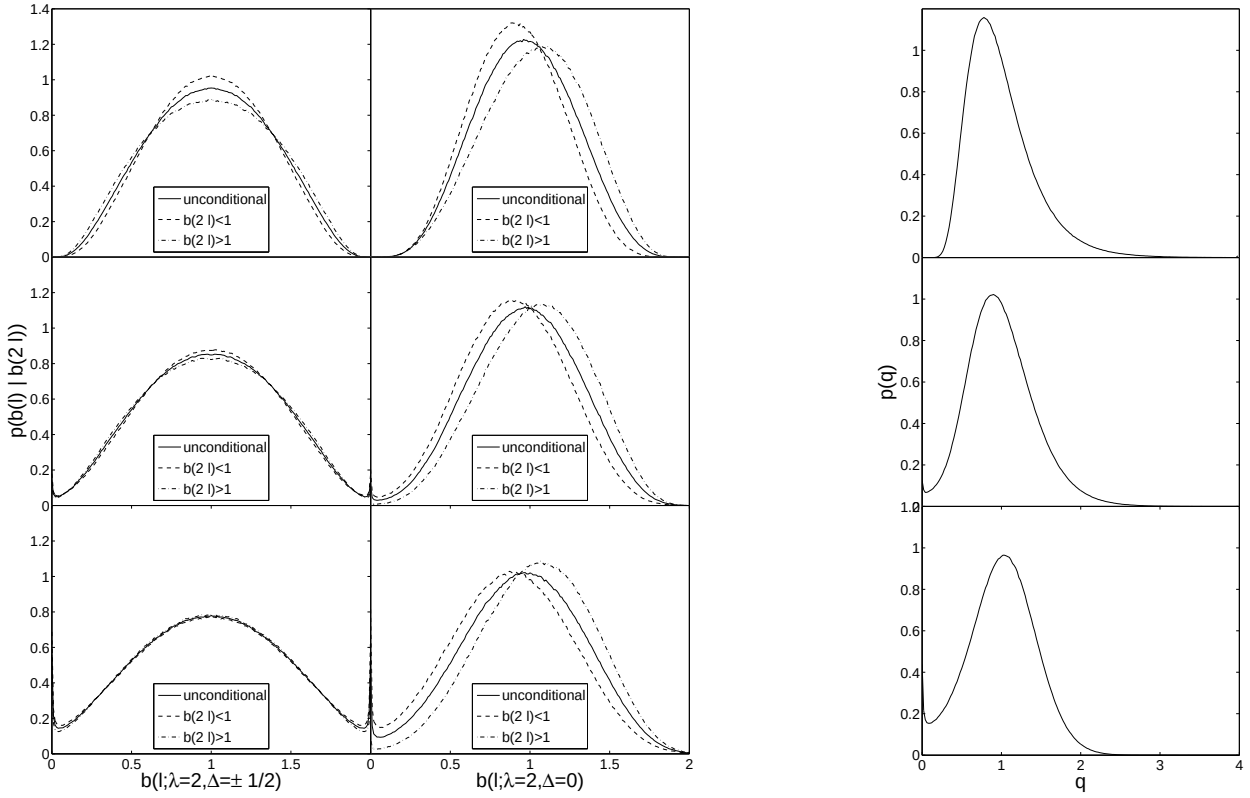

FIG. 2: Unconditional and conditional distributions of breakdown coefficients for $\lambda = 2$, $\Delta = \pm 1/2$ (first column), 0 (second column), at the typical scale $l = 32\eta$. From top to bottom row the stable index has been set to $\alpha = 2$, 1.7, 1.4. The intermittency exponent has been fixed to $\tau_2 = 0.24$. For comparison, respective log-stable distributions $p(q)$ for the random $\lambda = 2$ multiplicative weights of Eq. (3) are shown in the third column.

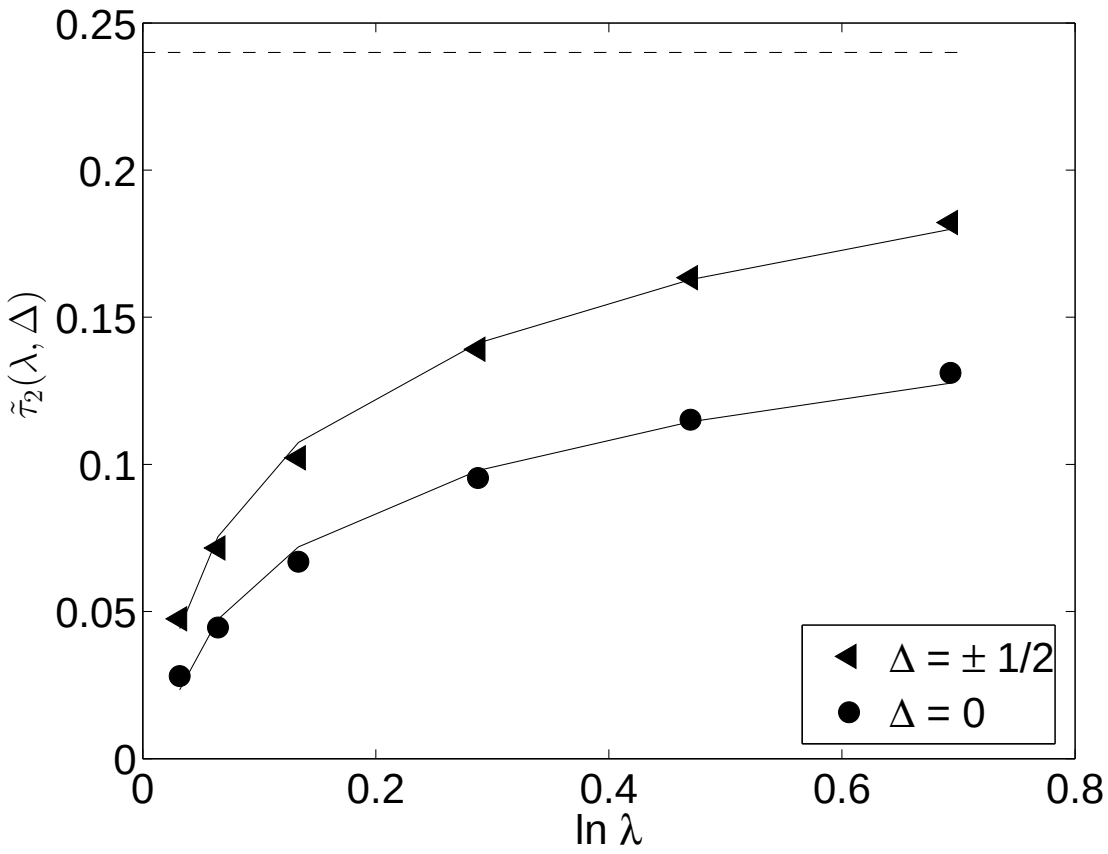

FIG. 3: Apparent intermittency exponent $\tilde{\tau}_2 = \ln\langle b^2(\lambda, \Delta)\rangle / \ln \lambda$ as a function of the scale ratio λ for $\Delta = \pm 0.5$ (triangle) and 0.0 (bullet). The second moment of the breakdown coefficients has been calculated for a typical length scale within the scale-independent regime. The solid curves represent a fit according to the suggestion (8) of Ref. [4]. For comparison, the dashed line shows the true $\tau_2 = 0.24$, which has served as model input.

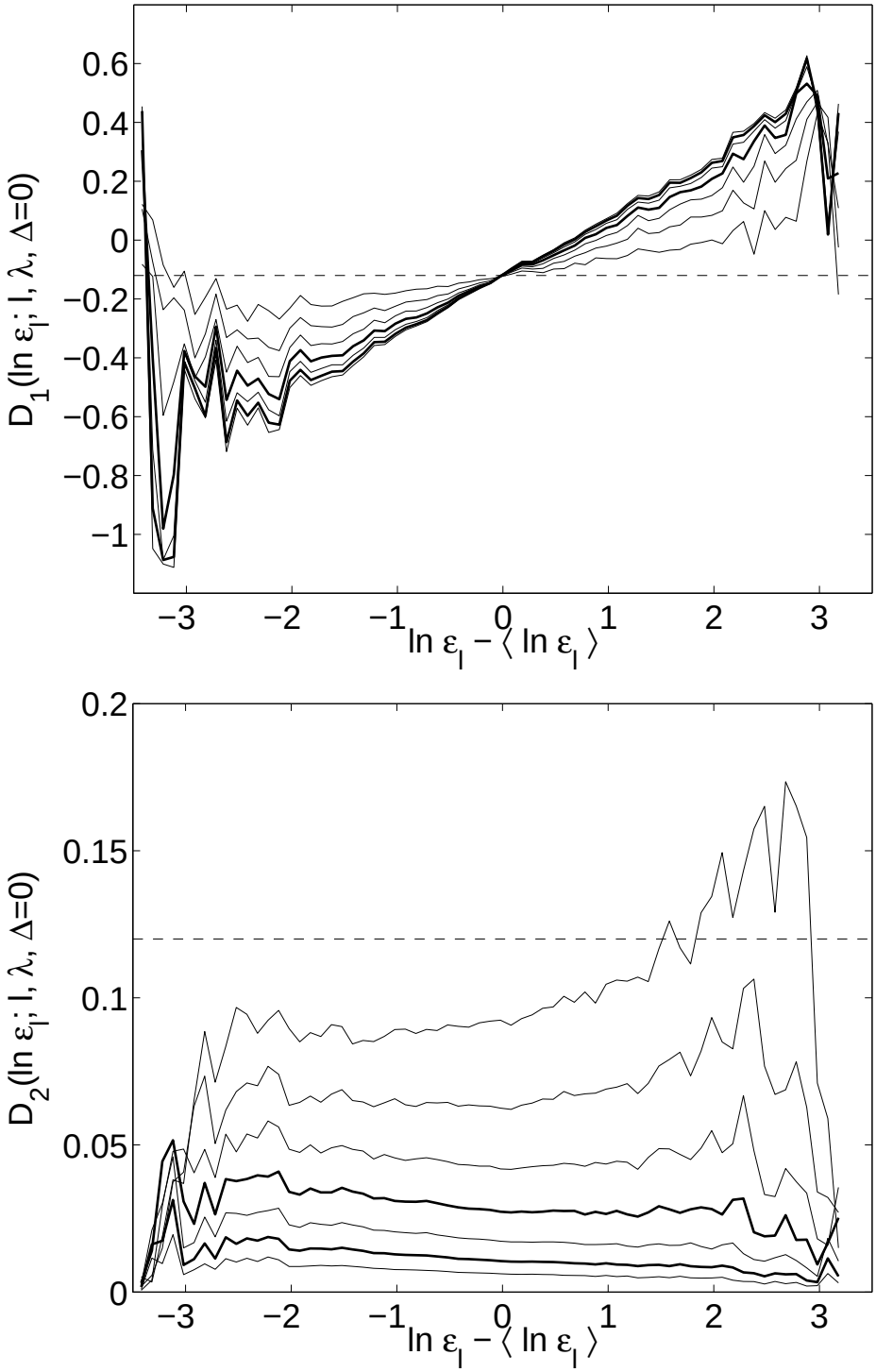

FIG. 4: Conditional first- (top) and second-order (bottom) moments $D_n(\ln \varepsilon_l; l, \lambda, \Delta)$ of breakdown coefficients for $\lambda = 2$, 4/3, 8/7, 16/15 (bold), 32/31, 64/63 (bold) and 128/127 (curves with increasing slope for D_1, and from top to bottom for D_2). Parameters are $\Delta = 0$ and, as a typical length scale, $l = 256\eta$. For comparison also the moments (12) and (13) (with $\lambda = 1$) are shown as dashed lines.

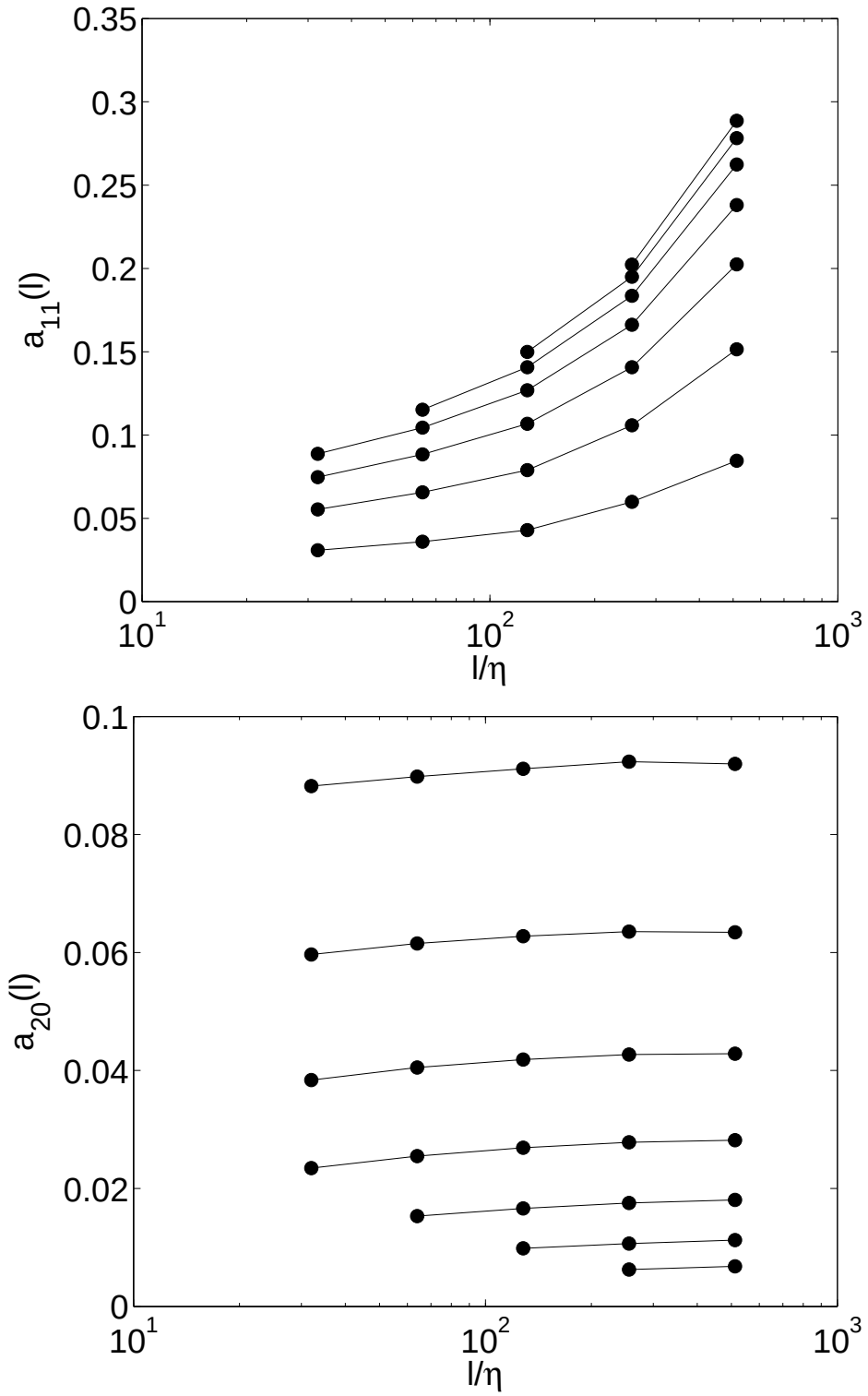

FIG. 5: Coefficients a_{11} (top) and a_{20} (bottom) of Eqs. (10) and (11) as a function of l for $\lambda = 2$, 4/3, 8/7, 16/15, 32/31, 64/63, 128/127 (a_{11}: from bottom to top, a_{20}: from top to bottom) and $\Delta = 0$.

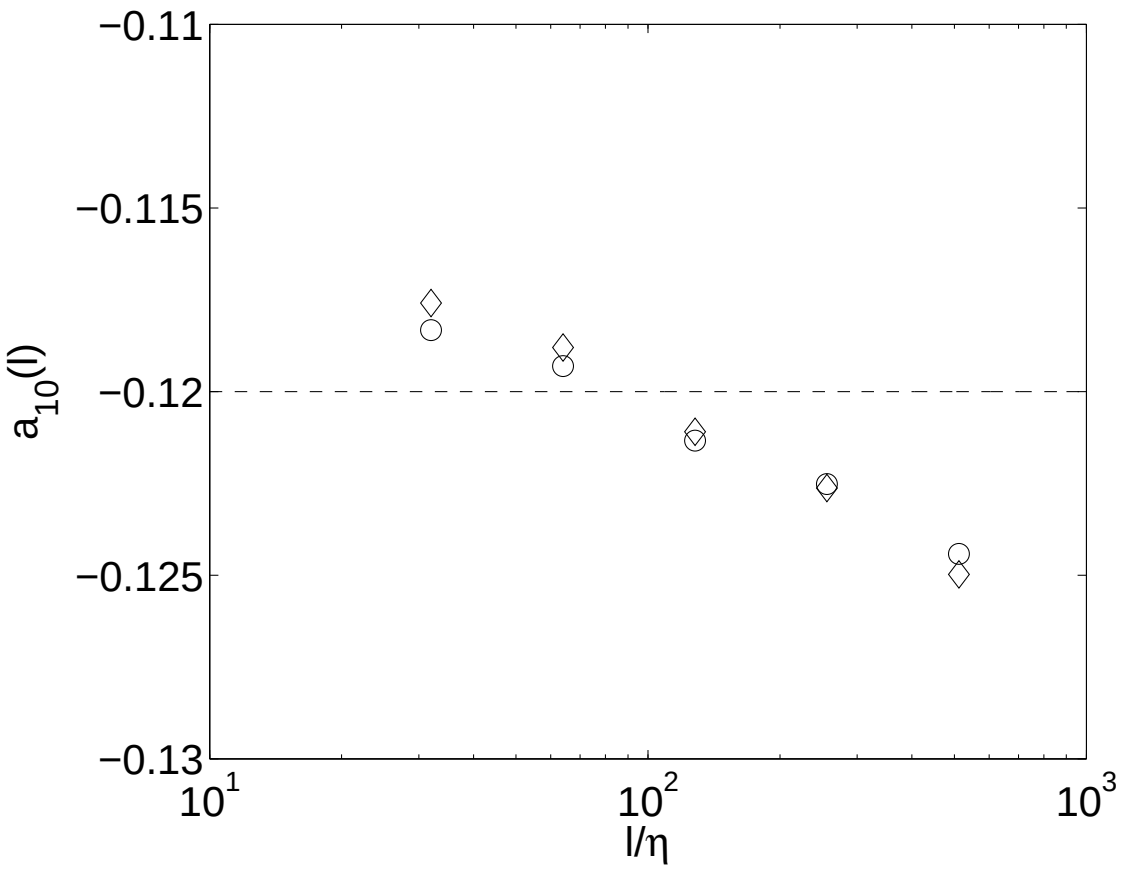

FIG. 6: The λ independent coefficient a_{10} of (10) as a function of the length scale l for $\Delta = 0$ (circles) and $1/2$ (diamonds). For comparison the constant (12) is shown as the dashed line.

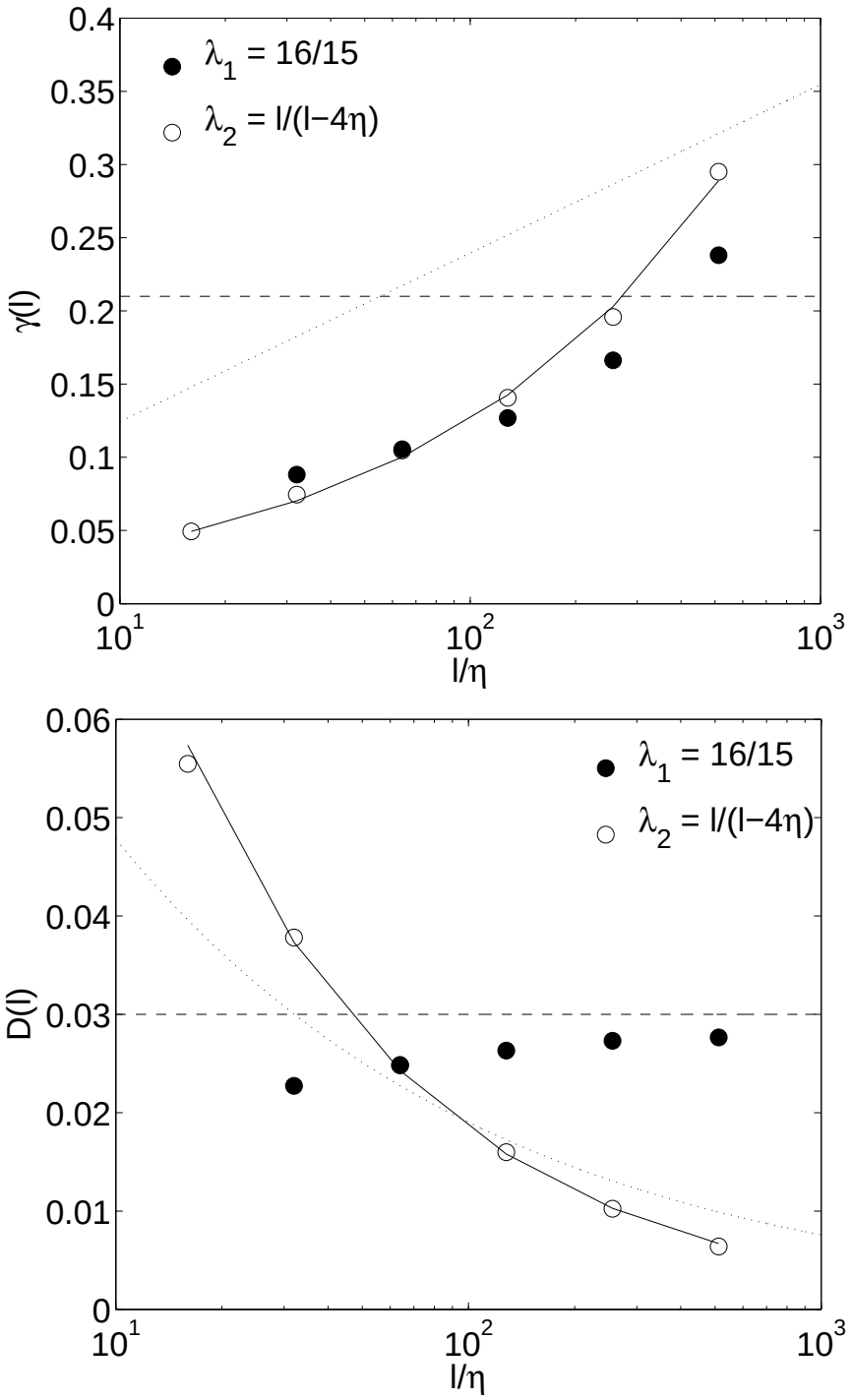

FIG. 7: (a) Drift coefficient $\gamma(l) = a_{11}(l, \lambda, \Delta = 0)$ and (b) diffusion coefficient $D(l) = a_{20}(l, \lambda, \Delta = 0)$ as a function of the length scale $16\eta \leq l \leq L$. The two operational definitions $\lambda_1 = 16/15$ and $\lambda_2 = l/(l - 4\eta)$ are shown with full and open circles, respectively. For the latter, the solid curves represent the parameterizations $\gamma(l) = 0.012(l/\eta)^{0.51}$ and $D(l) = 0.32(l/\eta)^{-0.62}$. For comparison, the λ_1 result (dashed) of Ref. [5] and the λ_2 result (dotted) of [6] are shown, which have been extracted from a low-temperature helium-jet flow.